Analysis of Permanent Magnet Synchronous Machines and Lundell Alternators Operating as Generators

Evandro Costa Souza
Matheus Henrique Rodrigues Miranda
Rosana Cibely Batista Rego
Ludmila Corrêa de Alkmin e Silva
Integrated Systems Laboratory, School of Mechanical Engineering – Universidade Estadual de Campinas – UNICAMP, Brazil.

ABSTRACT

The study of electric machines (EMs) used in the automotive industry has become crucial with the growing interest in electric and hybrid vehicles, driven by the need to reduce emissions, enhance performance, and improve energy efficiency. EM enables the regeneration of part of the energy that would otherwise be converted into heat during braking, allowing battery recharging and improving the overall system energy efficiency. In series hybrid vehicles, they can be used exclusively as generators, coupled to an internal combustion engine. In this work, we present a comparative study between two electric machines. For this purpose, a brief literature review on the principles of operation and mathematical modeling is conducted, as well as an analysis of the open-circuit voltage generation capacity of permanent magnet synchronous machines with axial flux and Lundell alternator, both operating as generators. The study is based on computational simulations, yielding an investigation into energy generation, which should be considered in various automotive applications.

Keywords: Lundell alternator; PMSM; synchronous generator; simulation; electric and hybrid vehicles.

INTRODUCTION

In recent years, the growing demand for energy-efficient and environmentally sustainable technologies has intensified interest in the analysis and application of electric machines (EMs), particularly in their operation as generators [1]. In applications such as Electric Vehicles (EVs) and Hybrid Electric Vehicles (HEVs), examining EMs as generators is essential for implementing regenerative braking and improving overall energy efficiency [1, 2]. Proper analysis of the generation mode allows optimal energy recovery, control of torque production, and management of battery charging dynamics. Additionally, understanding the generator behavior under varying speed and load conditions is necessary for designing effective control algorithms that ensure smooth transitions between motoring and generating modes, improve vehicle performance, and extend battery life [3, 4].

Among the various types of EMs, Permanent Magnet Synchronous Machines (PMSMs) and Lundell alternators stand out due to their general use in automotive and industrial applications [5, 6, 7]. Comprehending their operational principles and performance characteristics is crucial for improving energy conversion systems, optimizing control strategies, and advancing technological innovation in electric mobility and power generation [8].

PMSMs are known for their high efficiency, power density, and precise controllability, making them ideal for applications such as EVs and HEVs where performance and energy optimization are critical [9]. Their compact size and ability to operate efficiently across a wide range of speeds and load conditions have made PMSMs essential in achieving longer driving ranges and better overall system performance [10]. However, their reliance on rare-earth permanent magnets introduces concerns related to cost, thermal stability, and material sourcing [11]. On the other hand, the Lundell alternator, a widely used electromechanical generator in internal combustion engine (IEC) vehicles, represents a mature and cost-effective technology for DC power generation [12]. It is primarily used to supply power to the vehicle's electrical systems and to charge the battery. Although not as efficient or compact as PMSMs, Lundell alternators are valued for their robustness, cost-effectiveness, and ability to operate under the harsh thermal and mechanical conditions typical of automotive environments [12, 13]. In modern mild hybrid systems, modified versions of Lundell alternators, such as integrated starter-generators (ISGs), have been adapted to enable limited regenerative braking and engine start-stop functionality [14, 15].

The characterization of generator voltages is fundamentally important for the proper sizing of rectifiers, DC/DC converters, and frequency inverters. Therefore, mathematical models capable of accurately representing the behavior of the generated voltages play a decisive role in the selection and design of the most appropriate converter devices for electric vehicle applications [16, 17].

Inspired by the prior discussion, this paper presents a brief review of the operation of PMSMs and Lundell alternators operating as generators, with a focus on open-circuit conditions. The study of the PMSM was carried out using theoretical models, which were then confirmed through numerical simulation to show how the machine performs. In contrast, the analysis of the Lundell alternator was based on data from models developed by other researchers, since this work did not include direct experimental testing of the alternator.

BACKGROUND THEORY

LUNDELL'S ALTERNATOR – The Lundell's alternator is one of the most used electrical machines in vehicles with internal combustion engines due to its low cost, robustness, and wide operating speed range [18, 19]. The Lundell alternator is a three-phase synchronous machine with salient poles; however, due to the way the poles are distributed on the rotor, for analytical and modeling purposes, it can be assumed to have a smooth pole rotor [20]. The alternator has a rectifier coupled with its output, which may or may not be controlled, and its purpose is to recharge the vehicle's battery and supply energy to the vehicle's electronic systems. The electrical circuit that represents the Lundell alternator is shown in Figure 1.

Alternators can be self-excited through a secondary rectifier circuit at their output, which regulates the voltage to provide the field current. Some studies suggest different ways to increase alternator efficiency, such as replacing its field circuit with permanent magnets or operating at points of higher efficiency. Additionally, there are suggestions for rectifiers and power electronics systems with techniques that offer better performance [21, 22, 23, 24].

Any alterations, whether in its structural design or its electronic system, will result in increased production costs, making it less advantageous in terms of price.

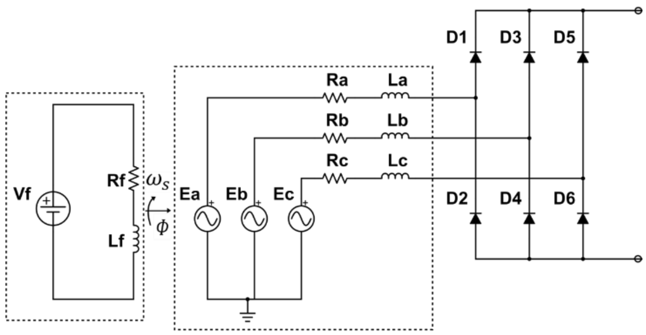

Figure 1: Representation of the electrical circuit of a Lundell alternator.

PERMANENT MAGNET SYNCHRONOUS MACHINE – PMSMs are synchronous electrical machines that, instead of having field windings on the rotor, use permanent magnets to provide machine excitation. These magnets produce a constant and rotating magnetic flux in the air gap at synchronous speed. The way the magnets are positioned on the rotor allows them to be classified as either radial or axial flux machines, as shown in Figure 2. Their advantages include high efficiency and high-power density [25]. As a type of rotary electrical machine, they can operate either as a motor or as a generator. However, when operating as a motor, they have a disadvantage regarding control, as they require a high-precision position sensor and high-performance processing [26].

The radial flux PMSM features a classic cylindrical geometry, in which the magnetic flux is distributed radially, that is, from the center of the rotor to the stator. The permanent magnets are mounted on the surface or embedded within the rotor, while the stator contains windings distributed in slots. The magnetic field generated by the magnets interacts with the rotating field of the stator, producing torque. This configuration is widely used due to its robustness, ease of manufacturing, and efficient control [27].

The axial flux PMSM, on the other hand, presents a disc-shaped architecture, where the magnetic flux is distributed along the axis of the motor. The magnets are mounted on rotating discs, positioned between flat stators or vice versa. The axial flux design allows for high torque density and thermal efficiency, making it ideal for applications where space and weight are limited, such as electric vehicles and drones [28, 29].

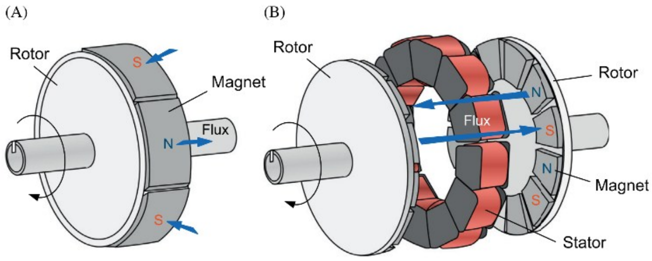

Figure 2: (A) Rotor of a radial flux PMSM, and (B) exploded view of a radial flux PMSM [25].

The following section presents a literature review on synchronous machines operating as generators.

SYNCHRONOUS GENERATOR – Synchronous machines are a type of rotating electrical machine in which alternating three-phase voltage is applied to the armature windings, but the magnetic field generated in the rotor can be produced by windings excited by DC (Direct current) or permanent magnets. Synchronous machines are commonly used as generators in hydroelectric plants, diesel generators, among others. The shape of their rotor may vary depending on the application; the cylindrical rotor can be used in high-speed situations, such as turbo generators, while salient pole rotors are better suited for lower speeds [31].

The rotating magnetic field in the stator is synchronized with the rotor speed, and therefore, there is no slip. The frequency of the voltage at the armature terminals (f_{se}) or stator is a function of the rotor speed (n_s) and the number of poles (P), and can be expressed by Eq. (1),

$$f_{se} = \frac{120*n_s}{P} \quad (1)$$

The voltage generated by a synchronous machine is a function of the magnetic field flux, its constructive aspects, and the rotational speed. For a synchronous generator excited through a field circuit, the induced voltage in phase A can be expressed by Eq. (2),

$$e_A = K\Phi\omega_e \tag{2}$$

where, e_A. represents the electromotive force in phase A, also referred to as EMF, K is a constant related to constructive aspects, and ω is the rotational speed in rad/s.
Eq. (2) can be simplified to express it as a function of the field current since the intensity of the field flux directly depends on the current in the rotor circuits. Therefore, the induced voltage in phase A can be written as,

$$e_A = K\omega_e i_f \tag{3}$$

where, i_f is the DC field current, thus not varying over time, and K represents the mutual inductance module associated with the reaction of concatenated fluxes between the armature and the field circuit [18]. Since the derivative i_f is zero, as it is a constant current, therefore non-variable over time, the voltage drops across the field inductance L_f can be disregarded, as its value is given by:

$$v_{L_f} = L_f \frac{di_f}{dt} \tag{4}$$

Therefore, the field current i_f is calculated as:

$$i_f = \frac{v_f}{R_f} \tag{5}$$

For a synchronous machine with permanent magnets, where the field flux is constant, the induced voltage can be represented as,

$$e_A = K\omega \tag{6}$$

The K constant continues to represent the constructive aspects of the machine and must consider the field flux promoted by the permanent magnets. Thus, the rotational speed of the shaft (ω) can be expressed in units of rad/s or revolutions per minute; this constant is provided by the manufacturer of the electrical machine.

The voltage E_A can be measured with the generator in an open circuit, as under this condition, there will be no voltage drop due to synchronous resistance and inductive reactance. The voltage in the other phases will have the same amplitude as E_A, but lagging by -120º and +120º concerning phase A, respectively, for E_B and E_C for positive phase sequence.

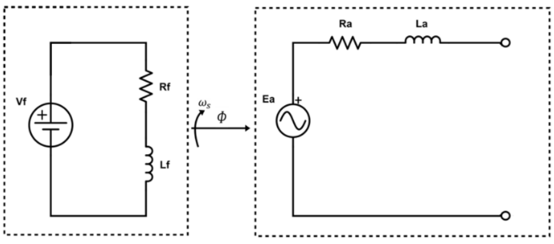

Figure 3: Electrical circuit representing the interaction between the field and armature windings.

The phase terminal voltage v_A can be calculated by subtracting the voltage drops across the resistance and synchronous inductance, thus,

$$v_A(t) = e_A(t) - R_A i_A(t) - L_A \frac{di_A(t)}{dt} \tag{7}$$

The voltage V_A can also be represented in the form of a phasor; therefore,

$$V_A = E_A - R_A I_A - jX_A I_A \tag{8}$$

Given V_A, E_A, and $I_A$are the phasors of the terminal voltage, induced voltage, and armature current, respectively. The reactance X_A can be calculated as:

$$X_A = 2\pi f_s L_A. \tag{9}$$

The value L_A does not behave as a constant and varies as a function of the interaction with the field flux. Reactance X_A is generally much greater than R_A, which allows ignoring the effects of R_A in some analyses.

The voltage across the synchronous reactance X_A can be calculated as,

$$v_{L_A} = L_A \frac{di_A(t)}{dt} \tag{10}$$

as presented in Eq. (7). However, the inductances must be represented considering the changes experienced due to the rotating magnetic field generated by the field flux, depending on the rotor position and the interaction with the other inductors in the machine. This introduces, in addition to its self-inductance, mutual inductances that depend on the interaction with the stator and field windings. Therefore, this voltage can be represented by the derivative of the concatenated flux λ, since $\lambda = li$. Thus, the voltage drops in the synchronous reactance of the winding corresponding to phase A can be expressed as:

$$v_{l_A} = \frac{d\lambda(t)}{dt} \tag{11}$$

Considering the mutual inductances due to electromagnetic interactions between the windings, the concatenated fluxes can be calculated from

$$\begin{bmatrix}\lambda_A\\ \lambda_B\\ \lambda_C\\ \lambda_f\end{bmatrix} = \begin{bmatrix}L_{AA} & L_{AB} & L_{AC} & L_{Af}\\ L_{BA} & L_{BB} & L_{BB} & L_{Bf}\\ L_{CA} & L_{CB} & L_{CC} & L_{Cf}\\ L_{fA} & L_{fB} & L_{fC} & L_{ff}\end{bmatrix} \times \begin{bmatrix}i_A\\ i_B\\ i_C\\ i_f\end{bmatrix} \tag{12}$$

Where L_{AA}, L_{BB}, L_{CC}, and L_{ff} are the self-inductances, and the other inductances represent mutual inductances for instance, L_{AB} represents the influence of the scattering flux generated by L_B on L_A.

As the mutual inductance between the stator and rotor varies according to the rotor's position at synchronous speed ω_s , its position θ_m, hence, the electrical position θ_e can be calculated considering the number of poles of the machine.

$$\theta_m = \omega_s t + \delta_0 \quad (13)$$

$$\theta_e = \left(\frac{polos}{2}\right)\theta_m + \delta_{e0} = \omega_e t + \delta_{e0} \quad (14)$$

Thus, the mutual inductance between the stator and rotor can be represented as a function of time variation. Therefore, the mutual inductance between the windings of phase A and the field circuit can be obtained from

$$L_{Af} = L_{fA} = L_{Af} cos\,(\omega_e t + \delta_{e0}) \quad (15)$$

The mutual flux between the stator and rotor of the other windings can be determined from the phase shifts of -120° and +120° for phases B and C, respectively. Thus, Eq. (7) can be rewritten as

$$v_A(t) = e_A(t) - R_A i_A(t) - L_A \frac{d\lambda_A(t)}{dt} \quad (16)$$

All the voltage values presented refer to the peak voltage in their respective phase; to find the effective voltage, it will be necessary to divide the peak voltage by $\sqrt{2}$. The armature windings of three-phase generators can be connected in star or delta configurations, thus, depending on how they are arranged, the line voltage can be calculated as,

$$\begin{aligned} V_{AB} &= \sqrt{3}|V_A|\angle\theta + 30° \\ V_{BC} &= \sqrt{3}|V_A|\angle\theta - 120° + 30° \\ V_{CA} &= \sqrt{3}|V_A|\angle\theta + 120° + 30° \end{aligned} \quad (17)$$

Equation 17 presents the line voltage at the generator terminals in a star connection; in a delta connection, the line voltage is equal to the phase voltage, thus, $V_{AB} = V_A$.
The input power can be calculated from the mechanical torque (τ_m), and rotation (ω_m) applied to the generator shaft, therefore,

$$P_{in} = \tau_m \omega_m \quad (18)$$

The mechanical power converted into electrical power inside the generator can be calculated as,

$$P_{conv} = \tau_{ind}\omega_m = 3E_A I_A\, cos\, cos\, \gamma \quad (19)$$

where γ is the angle between E_A and I_A,

The output power will be the mechanical input power minus the supplementary losses, friction losses, and core losses, which will result in the converted power. Subtracting copper losses from this will yield the power delivered to the load, as presented in Figure 4. The output power can be expressed as,

$$P_{out} = \sqrt{3}V_{AB} I_{AB}\, cos\, cos\, \theta = 3V_A I_A\, cos\, cos\, \theta \quad (20)$$

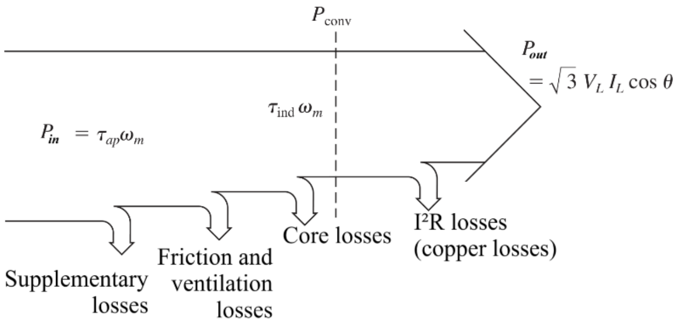

Figure 4: Relationship between input and output power and the losses involved. [32]

Therefore, the conversion efficiency (η) can be given by the ratio between the mechanical input power and the electrical power delivered to the load. Thus,

$$\eta = \frac{P_{in}}{P_{out}} \quad (21)$$

SIMULATION PARAMETERS

Due to the inability to determine the parameters of a Lundell alternator directly, the parameters established by Rodrigues [18] were adopted, and are presented on Table 1. However, for the PMSM, the data from the datasheet of an available test unit was used and are presented on Table 2.

Given the availability of a PMSM unit, validation tests will be conducted using this device. To gather open-circuit voltage data from the PMSM operating as a generator, a test bench was employed. This setup utilizes a brushless DC motor (BLDC) directly coupled to its shaft.

Table 1. Parameters of the Lundell alternator adapted from [18]

Parameter	Value
Number of poles (P)	16
Synchronous resistance (R_A)	0.03 Ω
Field resistance (R_f)	1.90 Ω
Synchronous inductance (l_A)	See equation 19
Field inductance (L_f)	0.2 H
Mutual inductance (K)	See equation 18
Diode conduction voltage (V_D)	0.8 V

Table 2. Parameters of the axial flux PMSM [35]

Parameter	Value
Nominal Voltage	250 V_{AC}
Nominal Power	55 kW
Nominal Torque	96 Nm
Maximum Speed	6500 rpm
Synchronous Resistance	1.35 mΩ
Inductance	15 µH

Parameter	Value
MMF vs. Rotational Speed Ratio (K)	0.0184 V_{RMS}/RPM
Number of Poles	20
Armature Windings Connection	Star

DISCUSSIONS AND RESULTS

LUNDELL ALTERNATOR – To perform the computational simulations presented in this work, the parameters used in the model are based on the study conducted by [20], which in turn was based on experimental data obtained from an alternator modeled by Sarafianos *et al*. (2015) [18] using experimental data. This work is limited to modeling the electrical circuit only, in order to analyze the behavior of the alternator under no-load conditions. Therefore, the electrical parameters of the alternator are defined as shown in Table 1.

Based on the characterization and parameter evaluation through experimental data by Sarafianos *et al*. (2015) [18], and analytical studies conducted by [3], it is possible to define the module of mutual inductance (K), for the mentioned alternator as:

$$K = 8.16 \times 10^{-3} \frac{-5.31\times10^{-3}}{1+10^{(2.9-i_f)3.87\times10^{-1}}} \quad (22)$$

And synchronous self-inductance can be defined as a polynomial function dependent on the field current, and is calculated as

$$l_A(i_f) = 2.35 \times 10^{-6} i_f^3 - 2.09 \times 10^{-5} i_f^2 + 1.96 \times 10^{-5} i_f + 2.96 \times 10^{-4} \quad (23)$$

Using the parameters presented in Table 1 and equations 18 and 19, it is possible to perform computational simulations that demonstrate the behavior of the terminal voltage of the alternator. Figure 5 shows the open-circuit output voltage values, considering an internal combustion engine of an HBEV (Hybrid Biofuel–Electric Vehicle) operating at the best trade-off point between emissions and energy consumption, with a rotation speed of 3000 rpm [33], coupled to the alternator through a 1:1 transmission ratio. To vary the voltage, a step of 0.2 A in field current was applied. In an open circuit, there is no voltage drop in the synchronous resistance and reactance, as there is no armature current. Therefore, the terminal voltage of the machine will match the electromotive force voltage (e_A) as presented in equation (5). Due to the presence of a full-wave three-phase rectifier at the alternator output, the rectified voltage can be determined from the peak value of the line voltage, V_{AB}, as presented in Eq. (24). Alternatively, if the effective phase voltage, $V_{A_{RMS}}$, is considered, the appropriate expression is given by Eq. (25).

$$V_o = \frac{3V_{AB}}{\pi} = 0.9549V_{AB} \quad (24)$$

$$V_o = \frac{3\sqrt{3}\sqrt{2}V_{A_{RMS}}}{\pi} = 2.3391V_{A_{RMS}} \quad (25)$$

The behavior of this system will change depending on the applied load; the terminal voltage will be reduced based on the armature current required by the load. The main purpose of the alternator is to recharge the battery; therefore, its output voltage must not exceed the maximum voltage supported by the battery and other electrical loads in the vehicle. Consequently, some commercial models will feature a system for voltage control and regulation, either through controlled rectifier bridges or DC/DC converters [34].

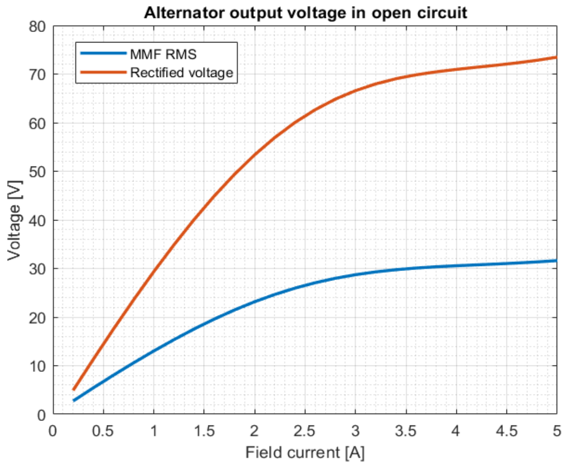

Figure 5: Alternator output voltage in open circuit before and after the rectifier bridge.

PERMANENT MAGNET SYNCHRONOUS MACHINE – To perform computational simulations representing the open-circuit voltage behavior of an axial flux PMSM, the parameters presented in Table 2 of a test-ready unit were considered.

An important piece of information in the simulation of electric machines is the field current. However, in PMSMs, there is no field current; instead, there is a constant air gap flux Φ, which allows for determining an equivalent field current value to use in the model. Thus, it is possible to use Eq. (8) to represent its behavior [30].

Different speeds were applied, and the voltage was measured using an oscilloscope. The curve representing the variation of the MMF measured at the machine terminals is shown in Figure 6.

To verify the relationship between the MMF and the rotational speed of the rotor shaft, the polynomial curve was plotted based on the measured data. The result was the first-order function:

$$e_A = 0.0183n_s + 0.0288 \quad (26)$$

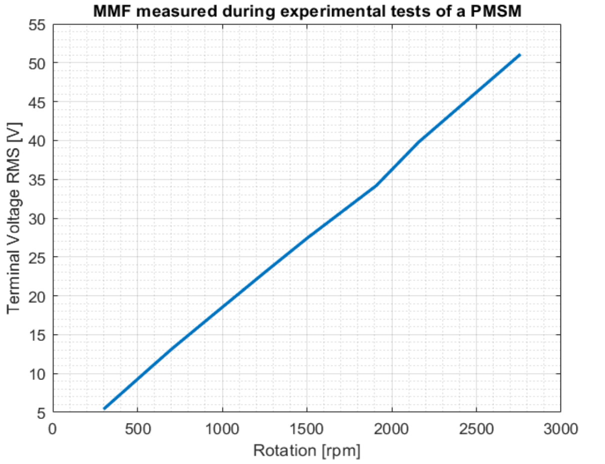

Figure 6: MMF measured during experimental tests of a PMSM

The error in the measured values was low, as can be seen in Figure 7. The angular coefficient of the line found for the polynomial curve fitting was 0.0183 V_{RMS}/RPM, very close to 0.0184 V_{RMS}/RPM presented in the PMSM datasheet. Therefore, it is possible to say that the model satisfactorily represented the behavior of the open-circuit voltage.

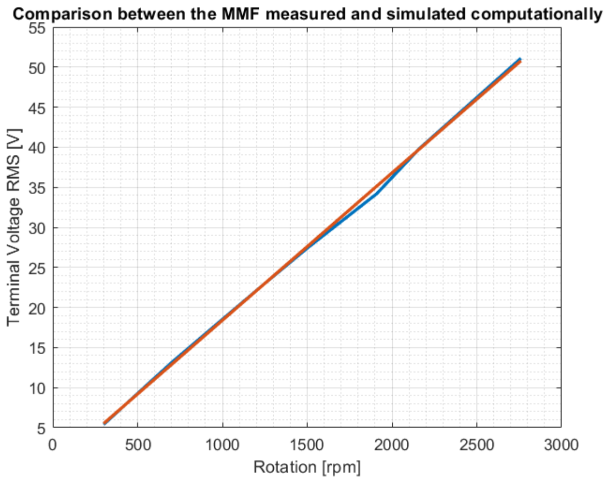

Figure 7: Comparison between the MMF measured and simulated computationally

CONCLUSION

The present study focused on performing computational simulations of MMF behavior in a Lundell alternator and an axial flux PMSM, which proved to be satisfactory and accurately represent the open-circuit MMF behavior. This information is crucial for designing energy generation systems in hybrid and electric vehicles and can contribute to the development of energy-efficient solutions.

It is a fact that the terminal voltage in a generator varies depending on the energy demand. Therefore, it is recommended that future studies consider these aspects, as well as mapping the efficiency of converting mechanical energy into electrical energy. For PMSMs, it is also interesting to consider their operation as a motor, applying traction force to a vehicle, in addition to studying their energy regeneration capacity. Validation of the models in bench tests is also suggested, along with adjusting the parameters of the electric machine based on experimental data. Additionally, mechanical and thermal models should also be considered.

ACKNOWLEDGEMENTS

This work was conducted with scholarships and financial support from Research Development Foundation - FUNDEP MOVER/Line V, from São Paulo Research Foundation - FAPESP (2021/14026-8), from Brazilian National Council for Scientific and Technological Development - CNPq (308389/2022-0), Incentive Program for New Professors at Unicamp – PIND (2500/23) and the Universidade Estadual de Campinas (UNICAMP).

REFERENCES

[1] Miguel-Espinar, Carlos, et al. "Review of flux-weakening algorithms to extend the speed range in electric vehicle applications with permanent magnet synchronous machines." IEEE Access 11, 2023, : 22961-22981.

[2] Barroso, Daniel G., et al. "Electrified automotive propulsion systems: state-of-the-art review." IEEE Transactions on Transportation Electrification 8.2, 2021, 2898-2914.

[3] Mustafi, Nirendra Nath. "An overview of hybrid electric vehicle technology." Engines and Fuels for Future Transport, 2021, 73-102.

[4] Cai, Shun, James L. Kirtley, and Christopher HT Lee. "Critical review of direct-drive electrical machine systems for electric and hybrid electric vehicles." IEEE Transactions on Energy Conversion, 2022, 2657-2668.

[5] Sangeetha, Elango, and Vijaya Priya Ramachandran. "An enhanced proportional resonance controller design for the PMSM-based electric vehicle drive system." Heliyon 10.15 (2024).

[6] Sain, Chiranjit, et al. "Self-controlled PMSM drive employed in light electric vehicle-dynamic strategy and performance optimization." IEEE Access 9 (2021): 57967-57975.

[7] Yu, Chia-Sung, Yuan-Chih Lin, and Ching-Jan Chen. "Rotational speed detection for the automotive alternator with low-loss rectifier in self-start." IEEE Transactions on Vehicular Technology 70.7 (2021): 6514-6526.

[8] Yazdan, Tanveer, Muhammad Humza, and Han-Wook Cho. "Three-phase dual-winding multitasked pmsm machine using double layer concentrated winding for HEV application." IEEE Access 11 (2023): 36682-36691.

[9] Pindoriya, Rajesh M., et al. "Numerical and experimental analysis of torsional vibration and acoustic noise of PMSM coupled with DC generator." IEEE Transactions on Industrial Electronics 69.4 (2021): 3345-3356.

[10] Sain, Chiranjit, et al. "Self-controlled PMSM drive employed in light electric vehicle-dynamic strategy and performance optimization." IEEE Access 9 (2021): 57967-57975.

[11] Cui, Jun, et al. "Manufacturing processes for permanent magnets: Part I—sintering and casting." Jom 74.4 (2022): 1279-1295.

[12] El-Hasan, Tareq. "Development of Automotive Permanent Magnet Alternator with Fully Controlled AC/DC Converter". Energies. 2018, 11. 274. 10.3390/en11020274.

[13] Tang, Sai Chun, Thomas A. Keim, and David J. Perreault. "Thermal modeling of Lundell alternators." IEEE Transactions on Energy Conversion 20.1 (2005): 25-36.

[14] Yushkova, O. A., et al. "Research on the Engineering Level of an Integrated Starter–Generator." Russian Electrical Engineering 95.12 (2024): 979-984.

[15] Viorel, Ioan-Adrian & Szabo, Lorand & Löwenstein, Lars & Şteţ, Cristian. (2004). Integrated Starter-Generators for Automotive Applications. 45.

[18] SARAFIANOS, Dimitrios; MCMAHON, Richard A; FLACK, Timothy J; PICKERING, Stephen. Characterisation and Modelling of Automotive Lundell Alternators. n. June, p.928–933, 2015.

[19] R. Bosch Gmbh, "Automotive Electrics Automotive Electronics", 5th ed. Wiley, 2007.

[20] G. S. L. Rodrigues, "Controle, gerenciamento e recuperação de energia em veículos a combustão interna," M.S. thesis, Centro de Engenharia Elétrica e Informática, Universidade Federal de Campina Grande, Campina Grande, 2019.

[21] R. Ivankovic, J. Cros, M. Taghizadeh, C. A., and P. Viarouge, 'Power Electronic Solutions to Improve the Performance of Lundell Automotive Alternators', New Advances in Vehicular Technology and Automotive Engineering. InTech, Aug. 01, 2012. doi: 10.5772/48459.

[22] S. C. TANG, D. M. OTTEN, T. A. KEIM and D. J. PERREAULT, "Design and Evaluation of a 42 V Automotive Alternator with Integrated Switched-Mode Rectifier," *2007 IEEE Vehicle Power and Propulsion Conference*, Arlington, TX, USA, 2007, pp. 250-258, doi: 10.1109/VPPC.2007.4544134.

[23] J. Rivas, D. Perreault and T. Keim, "Performance improvement of alternators with switched-mode rectifiers," in *IEEE Transactions on Energy Conversion*, vol. 19, no. 3, pp. 561-568, Sept. 2004, doi: 10.1109/TEC.2004.832072.

[24] Whaley, David & Soong, W. & Ertugrul, Nesimi. (2004). EXTRACTING MORE POWER FROM THE LUNDELL CAR ALTERNATOR.

[25] Noguchi, T. (2007), Trends of permanent-magnet synchronous machine drives. IEEJ Trans Elec Electron Eng, 2: 125-142. https://doi.org/10.1002/tee.20119.

[26] Huang Q, Huang Q, Guo H, Cao J. Design and research of permanent magnet synchronous motor controller for electric vehicle. Energy Sci Eng. 2023; 11: 112-126. doi:10.1002/ese3.1316.

[27] O. Bouaziz, I. Jaafar, and F. B. Ammar, "Performance analysis of radial and axial flux PMSM based on 3D FEM modeling," Turkish Journal of Electrical Engineering and Computer Sciences, vol. 26, no. 3, pp. 1587–1598, 2018.

[28] P. Curiac, "Optimum design aspects of a power axial flux PMSM," Revue Roumaine des Sciences Techniques – Électrotechnique et Énergétique, vol. 53, no. 1, pp. 31–39, 2008.

[29] J. Zhao, X. Liu, S. Wang, and L. Zheng, "Review of design and control optimization of axial flux PMSM in renewable-energy applications," Chinese Journal of Mechanical Engineering, vol. 36, no. 45, pp. 1–22, Apr. 2023.

[30] S.-H. Kim, "Electric Motor Control: DC, AC, and BLDC Motors", 1st ed., Amsterdam: Elsevier, 2017.

[31] S. D. Umans, "Máquinas elétricas de Fitzgerald e Kingsley", 7th ed., Porto Alegre, RS: AMGH Editora, 2014.

[32] S. J. Chapman, "Fundamentos de Máquinas Elétricas", 5th ed., Porto Alegre, RS: AMGH Editora, 2013.

[33] J. J. Eckert, F. L. Silva, S. F. da Silva, A. V. Bueno, M. L. M. de Oliveira, and L. C. A. Silva, "Optimal design and power management control of hybrid biofuel–electric powertrain," Applied Energy, vol. 325, p. 119903, 2022, doi: 10.1016/j.apenergy.2022.119903.

[34] D. J. Perreault and V. Caliskan, "Automotive power generation and control," in *IEEE Transactions on Power Electronics*, vol. 19, no. 3, pp. 618-630, May 2004, doi: 10.1109/TPEL.2004.826432.

[35] EMRAX, "EMRAX-228 Datasheet (v1.6)," Mar. 2025. [Online]. Available: https://emrax.com/wp-content/uploads/2025/03/EMRAX_228_datasheet_v1.6.pdf. [Accessed: May 13, 2025].